Realization of a near-perfect antireflection coating for silicon solar energy utilization

Mei-Ling Kuo,[1] David J. Poxson,[1] Yong Sung Kim,[1] Frank W. Mont,[2] Jong Kyu Kim,[2] E. Fred Schubert,[1,2] and Shawn-Yu Lin[1,*]

[1]*Department of Physics, Applied Physics and Astronomy, Rensselaer Polytechnic Institute, Troy, New York 12180, USA*

[2]*Department of Electrical, Computer, and System Engineering, Rensselaer Polytechnic Institute, Troy, New York 12180, USA*

**Corresponding author: sylin@rpi.edu*

Received June 12, 2008; revised August 20, 2008; accepted September 9, 2008; posted October 2, 2008 (Doc. ID 97248); published October 29, 2008

To harness the full spectrum of solar energy, Fresnel reflection at the surface of a solar cell must be eliminated over the entire solar spectrum and at all angles. Here, we show that a multilayer nanostructure having a graded-index profile, as predicted by theory [J. Opt. Soc. Am. **66**, 515 (1976); Appl. Opt. **46**, 6533 (2007)], can accomplish a near-perfect transmission of all-color of sunlight. An ultralow total reflectance of 1%–6% has been achieved over a broad spectrum, $\lambda=400$ to 1600 nm, and a wide range of angles of incidence, $\theta=0°-60°$. The measured angle- and wavelength-averaged total reflectance of 3.79% is the smallest ever reported in the literature, to our knowledge. © 2008 Optical Society of America

OCIS codes: 220.4241, 350.6050.

An antireflection (AR) coating is a type of coating applied to the surface of a material to reduce light reflection and to increase light transmission [1]. The coating can improve solar collection efficiency and, therefore, the overall solar-to-electricity efficiency. As solar radiation is broadband, the AR coating needs to be effective over the entire solar spectrum from ultraviolet and visible to IR wavelengths. To ensure high collection efficiency over an entire day, the coating also has to be effective for all angles of light incidence, θ. Hence, an ideal AR coating for solar application should maintain a low reflectance for all colors of sun light and all angles of incidence. However, the Fresnel reflection predicts a larger reflectance at larger θs, except for those near the Brewster angle. This presents a fundamental constraint against the requirement of a low reflectance at all angles.

A single layer of quarter-wave AR coating can give zero reflection at a specific wavelength (λ) [1]. However, it is effective only for a small λ range and a small θ range. A double layer AR coating has also been proposed to extend the range of low-reflectance regime $\lambda\sim450-700$ nm [2]. An alternative approach to increase the bandwidth is to create an artificially modified surface structure. For example, a periodic sub-λ surface structure was shown to suppress Fresnel reflection in the visible and near-IR at $\theta=0°$ [3]. It has been reported that a random silicon nanotip structure can give a total reflectance of less than 1% for $\lambda=0.2-2.5$ μm [4]. In their data, the authors might have removed the Si backside reflection of $\geqslant30\%$ at $\lambda>1.15$ μm, over which Si is optically transparent [3]. Although the process of random scattering can give a low total reflection over a large bandwidth, it is not as effective at larger θ [5]. Clearly, there is a need for an alternative AR-coating scheme for solar applications.

A theoretical calculation predicts an extremely low reflectance using the concept of a multilayer graded-index profile [6,7]. The design recognizes that the final reflectance of such an AR coating depends on the smoothness of the index profile. Mathematically, it is the differential reflectance at each interface of the multilayer structure that one must minimize to obtain a low final reflectance. As this minimization process does not depend strongly on λ or θ, it is intrinsically an all-θ and all-λ AR design. The all-θ and λ aspects of our graded-index nanostructure make it an ideal candidate for AR coating for solar utilization. Theoretical modeling of several types of graded-index profiles, including the quintic and Gaussian profiles, has predicted a low reflectance for broad λ ranges. The quintic profile is given by $n(z)=n_{\min}+(n_{\max}-n_{\min})(10z^3-15z^4+6z^5)$ [8]. For our AR coating, $n_{\min}(\text{air})=1$, $n_{\max}(\text{si})=3.6$, and z is the vertical optical distance measured from the air/AR-coating interface.

Experimentally, we grow a sequence of multilayer nanostructures to approximate the continuous index profile [9]. The multilayer AR coating is prepared by several deposition techniques that include the oblique angle deposition [10]. Briefly, the oblique angle deposition can produce slanted nanorods with a predesigned tilt angle and material porosity. A precise control of the porosity can lead to a controllable refractive index $n=1.09-2.6$ [11], allowing the realization of almost any graded-index profile. In Fig. 1, we show a SEM image of a graded-index AR-coating sample. The refractive indexes of each layer are char-

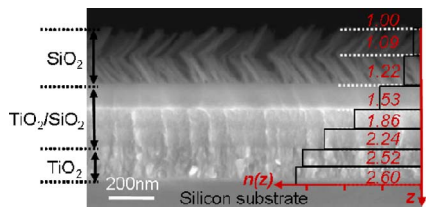

Fig. 1. (Color online) Scanning-electron-micrograph image of a seven-layer, graded-index AR-coating sample.

0146-9592/08/212527-3/$15.00 © 2008 Optical Society of America

acterized by ellipsometry, and their values are indicated. The thicknesses of each layer, from bottom to top, are 69, 78, 81, 101, 113, 145, and 156 nm, respectively. The bottom two layers are made of TiO_2. The middle three layers are cosputtered films using a combination of SiO_2 and TiO_2 to tailor the refractive index. The top two layers are made of slanted SiO_2 nanorods with very low refractive indexes of $n=1.22$ and 1.09, respectively. It will be shown that it is the combination of the graded-index profile and the extremely low index of the SiO_2 slanted rods that lead to a low reflectance and high transmittance over the entire solar spectrum.

To characterize the AR property of the graded-index coating, we measure its total reflectance, which is used to account for all the reflected light. The total reflectance measurements were performed for a broad range of (1) wavelengths ($\lambda=400-1600$ nm) and (2) incident angles, ($\theta=0°-60°$) as well as for the (3) TE and TM polarizations of light. The total reflectance is measured using a commercially available integrating sphere. For the λ-dependent study, several lasers were used, including $\lambda=454-514$ nm from an argon laser, $\lambda=633$ nm from a He–Ne laser, and $\lambda=780-1060$ and $\lambda=1260-1600$ nm from laser diodes. To study the θ dependence, the sample is mounted at the center of the sphere and the incident angle is varied by rotating the sample mount. The reflected light from the sample is collected by a calibrated silicon photodetector in the visible regime and an InGaAs detector in the near IR regime.

In Figure 2(a), we show the measured total reflectance spectra (the solid dots) for the bare silicon, the $\lambda/4$, and the graded-index samples. Light is incident at $\theta=8°$ and is TE polarized. The curves are from a theoretical calculation that accounts for the finite thickness of silicon substrate and its slightly rough back surface [12]. In brief, the silicon has a high reflectance of $R\sim31\%-49\%$, the $\lambda/4$ has a minimum reflectance at $\lambda=550$ nm and, finally, the graded-index sample has a low reflectance of $R\sim5\%$. However, all three samples exhibit an abrupt increase in their reflectance at $\lambda\sim1150$ nm, indicated by the vertical dashed lines. This sharp rise of reflectance may be attributed to the onset of silicon's optical transparency at $\lambda\sim1150$ nm, where silicon's indirect bandgap occurs [13]. In these λs, the portion of light passing through the AR coating is barely absorbed by silicon and would be reflected from the back surface of the silicon substrate [3]. In an attempt to quantify this effect, we first assume that the silicon substrate has no absorption in this regime $\lambda>1150$ nm. Second, we model the backside silicon–air interface as an optical flat surface with an effective index (n_{eff}) and an infinite thickness. This model calculation is accomplished using the transfer-matrix method (TMM) [12]. The model fit uses n_{eff} as a single fitting parameter. The model results (the solid curves) fit the data well and yield $n_{\text{eff}}=1.09$, 1.35, 1.09 for the backside of the silicon, $\lambda/4$ and graded-index AR coating samples, respectively. The satisfactory fitting indicates that the reflectance for $\lambda>1150$ nm comes from two contributions: one from the top surface and the other from the bottom surface.

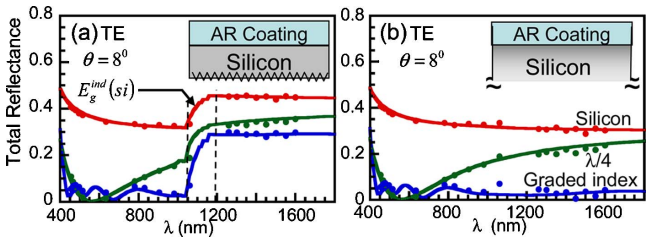

Fig. 2. (Color online) (a) Measured total reflectance spectra for the bare silicon (top curve), the $\lambda/4$ (middle curve), and the graded-index (bottom curve) AR-coating samples, respectively. (b) The deduced total reflectance data (solid dots) from the top AR-coating surface only.

After this analysis, the deduced experimental reflectance data (solid dots) from the top surface are plotted in Fig. 2(b). The silicon reflectance decreases monotonically as λ is increased, owing to a slight decrease in silicon's refractive index [14]. The $\lambda/4$ AR coating has super-low total reflectance of $R<3\%$ for a small bandwidth, $\lambda=550\pm50$ nm. But, beyond this λ range, reflectance increases rapidly and exhibits a strong λ dependence. For our graded-index AR coating, the total reflectance remains low, $R=1\%-6\%$, for all visible and near-IR wavelengths. The theoretical fits (the solid curves) in Fig. 2(b) are computed by assuming that the substrate is infinite to eliminate the contribution from backside reflection. The fitted result agrees well with the experimental data for all λ, except for $\lambda=1050$ nm, where silicon begins to become transparent. This data represents the first successful demonstration of an all-wavelength ($\lambda=400-1600$ nm) AR coating, having an ultralow reflection ($R=1\%-6\%$) for solar applications.

Next, we demonstrate the all-θ aspect of our graded-index AR coating while maintaining the broadband nature of the AR-coating. In Fig. 3, we plot the measured (dots) and calculated (curves) total reflectance of our graded-index sample versus θ for $\lambda=633$, 830, and 904 nm, respectively. The light is TE polarized. For comparison purposes, the total reflectance taken from a $\lambda/4$ AR coating is also shown. At $\lambda=633$ nm, both the graded index and $\lambda/4$ sample exhibit a similarly low reflectance at $\theta=8°$ and a reasonable reflectance of $R\sim10\%$ at $\theta=60°$. At λ

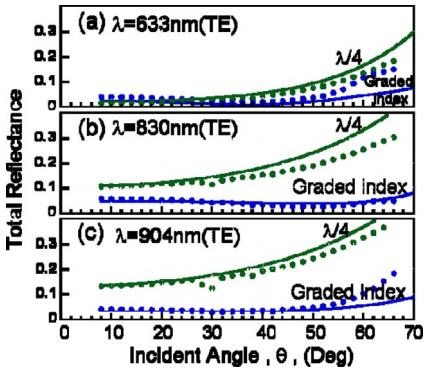

Fig. 3. (Color online) Comparison of total reflectance versus θ for the $\lambda/4$ and graded-index AR-coating samples at $\lambda=633$, 830, and 904 nm, respectively.

=830 nm, the total reflectance of our graded-index sample remains low ($R=2\%-5\%$) for all-θ. On the contrary, the total reflectance of a λ/4 sample becomes quite high, i.e., $R=11\%$ at $\theta=8°$ and $R=26\%$ at $\theta=60°$. At an even longer wavelength of λ=904 nm, our sample still maintains its low reflectance, while that for the λ/4 AR coating is much higher, $R=13\%-33\%$. This comparison illustrates the superior all-θ and all-λ aspect of our graded-index AR coating.

In the following, we compare the performance of our graded-index AR coating to a conventional λ/4 coating using the angle-averaged total reflectance. The angle-averaged total reflectance is defined using the following formula:

$$R_{angle\text{-}avg}(\lambda)=\frac{\int_8^{60}R(\theta,\lambda)\mathrm{d}\theta}{\int_8^{60}\mathrm{d}\theta}.$$

Here, the range of incident angles is limited by the testing setup. In Fig. 4(a), we present both the measured and calculated $R_{angle\text{-}avg}(\lambda)$ as a function of λ for TE polarization. Results of the TMM calculation reproduce the measured data well. Compared to the λ/4 coatings, our graded-index coating exhibits a much lower $R_{angle\text{-}avg}(\lambda)$ for the entire λ range and is nearly λ independent. In Fig. 4(b), we show $R_{angle\text{-}avg}(\lambda)$ for TM polarization, which exhibits a functional dependence very similar that for the TM polarization. For the bare silicon, the overall $R_{angle\text{-}avg}(\lambda)$ is lower for TM than that for TE polarization, owing to the occurrence of the Brewster angle for TM.

Finally, we compute the average total reflectance by integrating the fitted data, $R_{angle\text{-}avg}(\lambda)$, from λ =400 to 2000 nm for both polarizations, presented in Figs. 4(a) and 4(b), respectively. The results are summarized in Table 1. The average total reflectance over all angles and wavelengths of the bare silicon, λ/4 coating, and graded-index coating are 32.6%, 18.8%, and 3.79%, respectively. By conservation of energy, the total transmission efficiency of light and the total reflectance are related by $T_{Total}=1-R_{Total}$. Hence, the use of an graded-index and λ/4 coating can achieve solar collection efficiency (from λ=400–2000 nm) of 81.2% and 96.21%, respectively. This data illustrates that optical-to-electrical power conversion efficiency increases by 22.2% when going from a conventional single-layer λ/4 AR coating to a seven-layer graded-index AR coating.

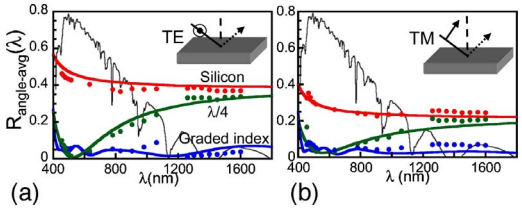

Fig. 4. (Color online) (a) Measured and calculated $R_{angle\text{-}avg}(\lambda)$ as a function of λ for TE polarization. The solar spectrum (thin curve) is shown as a reference. (b) $R_{angle\text{-}avg}(\lambda)$ for TM polarization.

Table 1. θ- and λ-Averaged Total Reflectance and Efficiency of AR Coating for Silicon, Single-Layer λ/4 Coating, and Graded-Index Coating Samples

	R_{avg} (%)	η of AR Coating (%)	Improved η over Silicon (%)
Silicon	32.6	67.4	
Single layer	18.8	81.2	20.5
Graded index	3.79	96.21	42.7

In summary, we have demonstrated a concept of multilayer AR coating that can be engineered to dramatically reduce optical reflection over all-λs of sunlight and incident angles. The graded-index approach offers a new mechanism for minimizing Fresnel reflection that is fundamentally different from either the traditional λ/4 AR coating or the modified surface structures. Further study of a more-robust porous film would be needed for a practicable solar cell application. The corresponding solar-to-electric efficiency over an uncoated silicon wafer is improved from 20.5% to 42.7% by going from a λ/4 coating to a seven-layer graded-index coating.

S. Y. L. acknowledges financial support from the Department of Energy–Basic Energy Services under grant DE-FG02-06ER46347.

References

1. G. R. Fowles, *Introduction to Modern Optics* (Dover, 1975), pp. 99–100.
2. V. M. Aroutiounuian, Kh. Martirosyan, and P. Soukiassian, J. Phys. D **39**, 1623 (2006).
3. Y. Kanamori, M. Sasaki, and K. Hane, Opt. Lett. **24**, 1422 (1999).
4. Y. Huang, S. Chattopadhyay, Y. Jen, C. Peng, T. Liu, Y. Hsu, C. Pan, H. Lo, C. Hsu, Y. Chang, C. Lee, K. Chen, and L. Chen, Nat. Nanotechnol. **2**, 770 (2007).
5. L. G. Shirley and N. George, Appl. Opt. **27**, 1850 (1988).
6. M. J. Minot, J. Opt. Soc. Am. **66**, 515 (1976).
7. M. Chen, H. Chang, A. S. P. Chang, S. Lin, J.-Q. Xi, and E. F. Schubert, Ophthalmic Physiol. Opt. **46**, 6533 (2007).
8. W. H. Southwell, Opt. Lett. **8**, 584 (1983).
9. S. R. Kennedy and M. J. Brett, Appl. Opt. **42**, 4573 (2003).
10. K. Robbie, M. J. Brett, and A. Lakhtakia, Nature **384**, 616 (1996).
11. J.-Q. Xi, J. Kim, E. F. Schubert, D. Ye, T.-M. Lu, and S. Lin, Opt. Lett. **31**, 601 (2006).
12. Z. Li and L. Lin, Phys. Rev. E **67**, 046607 (2003).
13. R. Poerschke and O. Madelung, *Semiconductors Group IV Elements and III-V Compounds: Data in Science and Technology* (Springer, 1991), pp. 12–13.
14. E. D. Palik, *Handbook of Optical Constants of Solid* (Academic, 1998), pp. 547–569.